Theor Chem Acc (2000) 105:15–30
DOI 10.1007/s002140000179

Theoretical
Chemistry Accounts

Regular article

Theoretical studies of isomers of C_3H_2 using a multiconfigurational approach

Mercedes Rubio[1], **Jonna Stålring**[2], **Anders Bernhardsson**[2], **Roland Lindh**[2], **Björn O. Roos**[2]

[1] Departamento de Química Física, Universitat de València, Dr. Moliner 50, Burjassot, 46100 Valencia, Spain
[2] Department of Theoretical Chemistry, Chemical Center, University of Lund, P.O. Box 124, 221 00 Lund, Sweden

Received: 25 January 2000 / Accepted: 26 April 2000 / Published online: 18 August 2000

Abstract. The C_3H_2 isomers are important molecules in interstellar space. An understanding of their electronic structure can contribute significantly to the interpretation of interstellar spectra. In a theoretical study of the C_3H_2 isomers a multiconfigurational treatment is of interest because many of the isomers are carbenes or diradicals. We present such an investigation of all possible C_3H_2 isomers. The most important features of their electronic and vibrational spectra are calculated. Earlier theoretical studies are reviewed and it is shown that the present study yields the same order of stability for the singlet and triplet states as most previous studies.

Key words: C_3H_2 – Isomerization – Complete-active-space self-consistent field – Multiconfigurational second-order perturburbation – Structures

1 Introduction

The "highly unusual" C_3H_2 isomers (Fig. 1) have been extensively studied since they have provided chemists with an intriguing problem of structure and chemical bonding. In particular, several of them represent the simplest parent species of their class, for instance, aromatic carbenes and cyclic alkynes. The detection of cyclopropenylidene (**1**) in the interstellar medium in 1985 led to a considerable increase in interest in the C_3H_2 isomers (Refs. [1–4] and references therein).

The first isomer identified was propargylene (**2**), which was shown to have a triplet ground state and a linear structure on the basis of the zero-field splitting parameters determined from the electron paramagnetic resonance (EPR) spectrum [5]. Two different structures have been considered for **2**: a 1,3-diradical form and an acetylenic carbene structure. Theoretical studies have predicted the two proposed structures for **2** to be nearly isoenergetic [1, 6, 7, 8]. The most extensive investigation of singlet **2** (**2s**) and triplet **2** (**2t**) was performed by Herges and Mebel [7]. On the basis of their quadratic configuration interaction (QCI) and multireference CI (MRCI) results, they concluded that **2t** has a 1,3-diradical structure with C_2 symmetry. The conclusion was also supported by the better agreement between the computed and experimental vibrational frequencies obtained for that structure [7]. In order to clarify the discrepancy with the earlier EPR experiment [5], which indicated a linear structure for **2**, Seburg et al. [9] subsequently reported the IR, UV/vis, and EPR spectra of this isomer. The study showed that the previous analysis of the geometry based on the zero-field splitting parameters was misleading owing to rotational motion of the molecule in the matrix [9]. The experimental EPR and IR spectra were consistent with a C_2 structure. Thus, high level ab initio calculations [7, 8] and the most recent experimental investigation agree with a 1,3-diradical C_2 structure for **2t**; however, there is no overall agreement between the computed and experimental IR spectra [7, 9].

Two other C_3H_2 isomers have been prepared in the laboratory: **1** and propadienylidene (**3**) [10, 11]. Theoretical calculations of the IR spectra played a significant role in the identification of both isomers, which have singlet ground states [12, 13]. In addition, it was shown that **1**, **2**, and **3** can be interconverted in a matrix by photolysis using light of different wavelengths [10, 11]. A detailed experimental investigation of the photochemical rearrangements on the C_3H_2 energy surface has recently been performed by Seburg and coworkers [9, 14]. As one of the results, the study suggests that the planar isomer of singlet cyclopropyne (**4s**) is the transition state for the automerization of **3**.

As far as we know, all possible singlet and triplet C_3H_2 isomers have been considered only in the early study performed by Hehre et al. [15] using single determinant ab initio methods. Subsequent studies have mainly focused on the most stable isomers and provide geometries, harmonic vibrational frequencies, and relative energies at different ab initio calculation levels [1, 4, 6–8, 14, 16]. Singlet **1**(**1s**) is predicted as the global

Correspondence to: B. O. Roos
(e-mail: bjorn.roos@teokem.lu.sc)

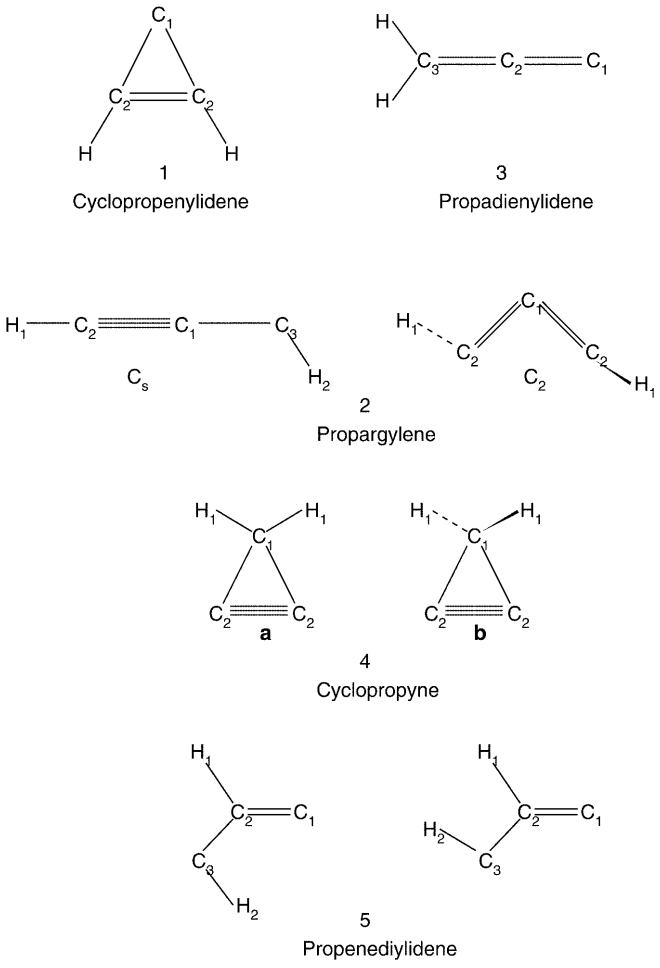

Fig. 1. The different isomers of C_3H_2 with the atom labeling

minimum on the C_3H_2 potential-energy hypersurface. **2t** and singlet **3** (**3s**) lie 10–11 and 12–14 kcal/mol, respectively, higher in energy, according to coupled-cluster results [14, 16, 17]. On the other hand, Mebel et al. [17] have recently investigated the isomerization mechanisms of C_3H_2 species using coupled-cluster and density functional methods as a preliminary step for understanding the photodissociation dynamics of allene and propyne (C_3H_4). Several theoretical studies on the electronic spectra of the most stable C_3H_2 isomers have also been reported [17–20].

Multiconfigurational (MC) methods are a priori expected to be more adequate for the study of the C_3H_2 potential-energy hypersurface since it contains carbenes and diradicals, as illustrated in Fig. 1, where several configurations can contribute significantly to the wave function [21, 22]. To go beyond single-configuration-based methods has been shown to be necessary in order to provide more definitive conclusions regarding the structure and relative energies of some C_3H_2 isomers [6, 7, 16]. As an example, Herges and Mebel [7] could only exclude the C_s carbene structure of **2t** on the basis of multireference CI results. It is therefore of interest to perform a complete study of the C_3H_2 potential-energy hypersurface using an MC approach. Furthermore, as stated earlier, all possible singlet and triplet geometries were only discussed by Hehre et al. [15] at the Hartree–Fock (HF)/STO-3G and Unrestricted HF (UHF)/STO-3G calculation levels. In this article, we present a detailed investigation of the singlet and triplet C_3H_2 isomers by means of the complete-active-space self-consistent-field (CASSCF) [23] and MC second-order-perturbation (CASPT2) methods [24, 25]. The study includes geometry optimizations and vibrational frequency calculations for the singlet and triplet states of each isomer, as well as the determination of singlet–triplet energy differences. The relative isomer stability is also discussed. For the most stable isomers, the investigation has been extended to the lowest excited states. The results obtained in the present work allow us to assess the performance of single-configuration-based methods to describe the C_3H_2 potential-energy hypersurface.

2 Methods and calculation details

The CASSCF [23] and CASPT2 [24, 25] methods were used in the present work. The CASSCF method is a particular case of a more general MC SCF method. The wave function is constructed as a superposition of all configurations which can be formed by distributing a certain number of electrons among a given set of active orbitals, restricted only by point group and spin symmetry. The CASPT2 method [24, 25] provides a second-order estimate of the remaining correlation energy (dynamic) based on a CASSCF reference function.

The full valence active space of C_3H_2 isomers consists of 14 orbitals and includes 14 electrons. In all the CASSCF calculations, the three core orbitals and the deepest valence totally symmetric orbital were kept inactive. In addition, a weakly occupied orbital belonging to the totally symmetric irreducible representation of the corresponding point group was moved to the virtual space. The full valence active space was in this way reduced to 12 orbitals with 12 electrons active. All geometry optimizations were performed at the CASSCF level of theory, using the MOLCAS gradient facility. A recently developed program to compute second-order MCSCF derivatives [26] was used in order to determine the type of stationary points found on the CASSCF potential energy hypersurface. Harmonic vibrational frequencies and zero-point vibrational energies (2PVE) were calculated for the singlet and triplet states of each isomer at the CASSCF level.

Total energies were computed at the CASPT2 level, without including correlation of the core electrons. The CASPT2 calculations were performed using a zero-order Hamiltonian with the one-particle Fock operator modified by the $\mathbf{g}_1$ operator [27] since it provides a better estimate of singlet–triplet energy differences. For methylene (CH_2), the CASPT2 value for the singlet-triplet separation is overestimated by 1.2 kcal/mol compared to the full CI result when the $\mathbf{g}_1$ correction and a valence active space are used in the calculations [27].

Generally, contracted basis sets of atomic natural orbital (ANO) type were used; these were obtained from the C(10s6p3d)/H(7s3p) primitive sets [28]. Two contraction schemes, C[3s2p1d]/H[2s1p] and C[4s3p2d]/H[3s2p], were used for geometry optimizations and the calculations of harmonic vibrational frequencies, which are denoted as BS1 and BS2, respectively. An ANO type basis set constructed from a larger number of primitive functions, C(14s9p4d3f)/H(8s4p3d) [29], and contracted to C[5s3p2d1f]/H[3s2p1d] was used for single-point energy calculations in order to provide more accurate relative energies. This basis set is denoted BSL.

All calculations were performed with the MOLCAS-4 quantum chemistry software [30]. Harmonic vibrational frequencies were computed with the recently developed McKINLEY and MCLR programs [26].

3 Results and discussion

As a first step in the present study, we examined all possible singlet and triplet C_3H_2 isomers as Hehre et al. [15] did. Full geometry optimizations within the symmetry restrictions imposed by the symmetry group to which each type of structure belongs were performed at the CASSCF level using the C[3s2p1d]/H[2s1p] basis set (CASSCF/BS1 results). Each stationary point found was then characterized on the basis of the harmonic vibrational frequencies computed at the same level of theory. As expected, structures **1** and **3** were predicted to be a minimum on the singlet surface. For **2s**, only the C_s structure (Fig. 1) was found to be a minimum, while the corresponding C_2 structure is a transition state. **4** was also characterized as a transition state on the singlet surface in both planar (**4a**) and perpendicular (**4b**) geometries. The optimization of singlet propenediylidene (**5s**) led to structure **1**, the global minimum of the singlet surface, as found in previous studies [14, 15]. A larger number of structures were predicted to be minima on the triplet surface: **2t**, in both C_s and C_2 geometries, **3t**, **1** with an unsymmetrical structure, **4t** with the tetrahedral carbon (perpendicular structure), and **5t**.

The relative energies of the isomers were calculated at the CASPT2 level of theory, using the ANO-L BSL basis set and CASSCF/BS1 optimized geometries (CASPT2/BSL results). Unless otherwise stated, all the electronic energy differences were obtained at the CASPT2/BSL level. More attention was paid to the most stable isomers where the study was extended to the lowest excited states. Finally, in order to get more accurate harmonic vibrational frequencies, the geometries of the lowest singlet and triplet states of each isomer were reoptimized using the larger C[4s3p2d]/H[3s2p] basis set (CASSCF/BS2 results), and the frequencies and IR intensities were recomputed.

In the following, we shall first focus on the results obtained for each structure separately. The relative energies of the isomers will then be discussed and compared with previous theoretical results. Finally, the computed harmonic vibrational frequencies and IR intensities are presented and compared with the available experimental and other ab initio predicted IR spectra.

3.1 Cyclopropenylidene

1 is the smallest aromatic carbene and the most stable C_3H_2 isomer. It was first detected in the laboratory in 1984 by Reisenauer et al. [10] via matrix isolation. The theoretically predicted IR spectrum aided in its identification [12]. The present work includes the ground and low-lying electronic states.

The CASSCF optimized geometries for the 1^1A_1 ground state and the lowest singlet and triplet A_2 and B_1 states are collected in Table 1. C_{2v} symmetry was imposed in the optimizations. For the sake of comparison, the coupled-cluster singles–doubles and perturbative triple excitation [CCSD(T)] and Becke's three parameter hybrid with the Lee, Yang, and Pam correlation functional (B3LYP) optimized geometries for the ground state [16, 17] and the experimental data [31] are also included. As can be seen, all theoretically predicted geometries for the 1^1A_1 state are quite similar and also agree with the experimental geometry determined from the microwave spectrum [31]. For instance, the C—C bond lengths computed at the CASSCF/BS2 level differ by less than 0.01 Å from the CCSD(T) values [16]. The influence of the basis set on the CASSCF bond lengths is less than 0.015 Å. For the excited states, the restricted open-shell HF (ROHF) optimized geometries reported by Bofill et al. [18] are included in Table 1. As could be expected, the bond lengths computed at the ROHF/3-21G level are, in most cases, shorter (0.02–0.06 Å) than

Table 1. Bond lengths (Å) and angles (°) for the ground and lowest excited states of cyclopropenylidene, **1**, compared to other ab initio results. Atom numbering according to Fig. 1. Note here that the C_{2v} geometries of the excited states are not minimum energy structures (see text for details)

Method	C_1—C_2	C_2—C_2	C_2—H	C_2—C_1—C_2	C_1—C_2—H
1^1A_1 ground state					
CASSCF/BS1	1.433	1.347	1.103	56.1	147.8
CASSCF/BS2	1.419	1.335	1.090	56.1	147.4
CCSD(T)/TZ(2df,2pd)[a]	1.427	1.328	1.076	55.5	149.8
B3LYP/6-311G(d,p)[b]	1.423	1.323	1.080	55.4	147.7
Experiment[c]	1.420	1.324	1.075	55.6	148.0
1^3A_2 state					
CASSCF/BS1	1.363	1.636	1.094	73.7	160.8
CASSCF/BS2	1.350	1.630	1.081	74.3	160.9
ROHF/3-21G[d]	1.343	1.579	1.053	72.1	157.9
1^1A_2 state					
CASSCF/BS1	1.365	1.605	1.094	72.0	155.6
ROHF/3-21G[d]	1.343	1.564	1.054	71.3	155.9
CASSCF/6-311(d,p)[b]	1.337	1.537	1.061	70.2	156.5
1^3B_1 state					
CASSCF/BS1	1.472	1.355	1.101	54.8	150.5
ROHF/3-21G[d]	1.477	1.311	1.059	52.7	149.7
1^1B_1 state					
CASSCF/BS1	1.476	1.389	1.100	56.2	156.1
ROHF/3-21G[d]	1.484	1.334	1.060	53.4	152.4

[a] Ref. [16]
[b] Ref. [17]
[c] Microwave structure (r_s values) from Ref. [31]
[d] Ref. [18]

the CASSCF values. The 1^1A_2 state has also been optimized at the CASSCF level by Mebel et al. [17], resulting in C—C bond lengths even shorter than the ROHF values, as can be seen in Table 1. The differences with respect to our results are probably related to the active space, which consisted of eight electrons distributed in ten orbitals in the CASSCF calculations performed by Mebel et al. [17] compared to the 12 orbitals and 12 electrons included here.

The CASPT2 relative energies of the lowest excited states of **1** are shown in Table 2 together with other ab initio results. As all theoretical studies predict [6, 12, 15, 18], **1** has a closed-shell singlet 1^1A_1 ground state. Two different effects contribute to stabilize the singlet ground state. On the one hand, the small angle at the carbene center, imposed by structural considerations, decreases the energy of the σ lone-pair orbital. On the other hand, the π orbital on the divalent carbon is raised in energy owing to the interaction with the π orbital of the ethylene substituent. Therefore, the 1^1A_1 state is aromatically stabilized, which is reflected in the geometry of the molecule (Table 1). The values 1.419 and 1.335 Å are predicted for the single-bond and double-bond lengths, respectively, at the CASSCF/BS2 level, illustrating the electron delocalization in the ring.

Computed energies for the 1^3A_2 and 1^1A_2 states are 54.6 and 58.1 kcal/mol, respectively, above the ground state. They are mainly described by the one-electron promotion from the σ lone-pair orbital at the carbene center to the antibonding π orbital of the ethylene part of the molecule. The singlet and triplet A_2 states have similar geometries, which are, however, quite different from the ground-state structure. Thus, the angle at the carbene center increases (16–18°) and the C—C single-bond lengths decrease and become closer to the length of a double bond. The vibrational frequencies show that these C_{2v} structures of the A_2 states are not stable, in agreement with previous studies [8, 12, 18]. Two imaginary frequencies corresponding to normal modes of b_1 and a_2 symmetries (out-of-plane CH bend) were obtained. Earlier studies using the SCF method also predicted a third imaginary frequency related to the breaking of one of the two equivalent C—C bonds [12, 18]. Bofill et al. [18] performed geometry optimizations for the A_2 states without symmetry constraints at the SCF level. A highly unsymmetrical structure was characterized as a true minimum for both singlet and triplet A_2 states. These authors attributed the unsymmetrical equilibrium geometries to HF instability of the ROHF wave functions of the A_2 states and suggested that a MCSCF treatment could solve the problem and provide a stable C_{2v} geometry [18]. Subsequent CASSCF optimizations for the lowest triplet state of **1** predicted, however, an unsymmetrical structure [6]. The present results of the vibrational analysis agree with a recent coupled-cluster study [8], which also resulted in two imaginary frequencies related to b_1 and a_2 normal modes for the C_{2v} structure of the lowest triplet state, leading to an unsymmetrical structure as the most stable.

In order to provide an equilibrium geometry for the lowest triplet state of **1**, we also carried out a full geometry optimization without symmetry constraints. The optimal bond lengths and bond angles are given in Table 3 and are compared to the CCSD(T) values reported by Ochsenfeld et al. [8]. The vibrational analysis showed that this unsymmetrical structure is a minimum on the triplet C_3H_2 energy surface (vide infra), in agreement with the coupled-cluster results [8]. Compared to the C_{2v} geometry (Table 1), the distortion results in a lengthening of one of the C—C double bond lengths (C_1—C_3 in Table 3) and a movement out of the plane of the corresponding hydrogen atom (H_2). The electronic structure can be approximately described as a diradical with the electrons localized in C_1 and C_3 [CASSCF/BS1 spin density values are: 0.7(C_1), 0.2(C_2), and 1.1(C_3)]. The decrease in energy produced by the distortion is 5.1 kcal/mol, to be compared with the value of 6.3 kcal/mol reported by Ochsenfeld et al. [8] at the CCSD(T) level. The present results locate the lowest triplet state of **1** 49.5 kcal/mol above the ground state.

The 1^3B_1 state was computed to be 64.6 kcal/mol above the ground state, close in energy to the A_2 states, as can be seen in Table 2. This state is mainly described by the one-electron promotion from the σ lone-pair

Table 2. Computed relative energies (kcal/mol) for the lowest states of **1** compared to other ab initio results. All calculations at the complete-active-space self-consistent-field (*CASSCF*)/BS1 optimized geometries within C_{2v} symmetry

State	CASPT2	μ[a] (D)	MRCI + D[b]	CISD/6-31G*[c]
1^1A_1	0.0	3.42	0.0	0.0 (3.07)[d]
1^3A_2	54.6	1.55		66.4 (1.02)
1^1A_2	58.1	0.89	57.6	70.1 (0.60)
1^3B_1	64.6	1.56		69.9 (1.42)
1^1B_1	99.5	2.87	103.8	119.0 (2.64)

[a] Dipole moment computed at the CASSCF level with the BSL basis set
[b] Adiabatic excitation energies from Ref. [17]. A C_s geometry is predicted for the 1^1B_1 state
[c] Ref. [18]. Values estimated assuming additivity of the electron correlation and polarization corrections. Dipole moments computed at the SCF/6-31G* level are shown in *parentheses*
[d] Result obtained from a TCSCF wavefunction, Ref. [18]

Table 3. Minimum energy structure optimized for the lowest triplet state of **1**. C_1 is characterized by not holding hydrogen atoms

	CASSCF/BS1	CASSCF/BS2	CCSD(T)/TZP[a]
Bond lengths (Å)			
C_1—C_2	1.304	1.314	1.304
C_1—C_3	1.499	1.480	1.448
C_2—C_3	1.578	1.574	1.551
C_2—H_1	1.099	1.061	1.073
C_3—H_2	1.114	1.100	1.088
Angles (°)			
C_3—C_1—C_2	68.1	68.3	
C_1—C_3—C_2	50.1	50.9	
C_1—C_2—H_1	156.7	158.4	
C_1—C_3—H_2	128.7	129.3	
C_1—C_3—C_2—H_1	178.1	178.0	
C_2—C_1—C_3—H_2	107.0	107.0	

[a] Ref. [8]

orbital to the π orbital at the carbene center. The corresponding singlet state is located at higher energies: 99.5 kcal/mol. As regards the geometry, the results collected in Table 1 show that both singlet and triplet B_1 states have C_{2v} structures quite similar to the ground-state geometry; however, according to the present harmonic vibrational analysis, the C_{2v} structures of the B_1 states do not correspond to equilibrium geometries, as was previously suggested on the basis of the force constants determined at the HF level [12, 18]. Thus, the CASSCF optimized structure for the 1^3B_1 state (Table 1) has one imaginary frequency corresponding to a normal mode of b_2 symmetry, which is mainly related to the asymmetric C—C stretch. The CASSCF harmonic vibrational frequencies computed for the 1^1B_1 state also show one imaginary frequency which corresponds to the out-of-plane and in-phase C—H bend (normal mode of b_1 symmetry).

The singlet excited states of **1** have recently been studied by Mebel et al. [17]. The study included geometry optimizations at the CASSCF level, the calculation of vibrational frequencies by means of the singles CI (CIS) method, and vertical and adiabatic excitation energies computed using the MRCI approach. These authors reported a stable C_{2v} structure for the 1^1A_2 state, with no imaginary frequencies at the CIS level, in contrast with the two imaginary frequencies obtained at the CASSCF level in the present study (vide supra). As regards the 1^1B_1 state, Mebel et al. [17] also predicted the C_{2v} geometry to be unstable, with one imaginary frequency related to a mode of b_2 symmetry instead of the b_1 mode found here. These authors then performed a CASSCF optimization within C_s symmetry, which resulted in a slightly distorted C_{2v} structure for the 1^1B_1 state. As can be seen in Table 2, the adiabatic excitation energies reported by Mebel et al. [17] at the MRCI level are in line with the CASPT2 values which were obtained using the CASSCF/BS1 optimized geometries within C_{2v} symmetry (Table 1). Summarizing, the lowest singlet and triplet excited states of **1** do not have equilibrium geometries of C_{2v} symmetry, namely, **1**-like geometries. A totally unsymmetrical structure was predicted for the lowest triplet state, in agreement with a recent coupled-cluster study [8].

3.2 Propadienylidene

3 can be considered as the simplest vinylidenecarbene. This C_3H_2 isomer was first observed in the laboratory by Maier et al. [11] in 1987. From the IR and EPR spectra, it was clearly established to have a singlet ground state and an allene-like structure [11], in agreement with the theoretical predictions [1, 6, 15]. The electronic absorption spectrum of **3** has recently been reported and interpreted on the basis of coupled-cluster calculations [19]. In addition, the singlet excited states have been extensively studied by Mebel and coworkers [17, 20] because of their possible implications in the photodissociation dynamics of allene.

The present investigation of **3** focused on the ground and low-lying singlet and triplet excited states. The CASSCF optimized geometries for the states considered are presented in Table 4 and are compared with other theoretical results. The geometries were fully optimized with the constraint of C_{2v} symmetry. All the states were found to have a C_{2v} equilibrium geometry, except the 1^1A_2 state. The computed adiabatic excitation energies are given in Table 5 and are related to available experimental data [19, 32]. As stated previously, the CASPT2 electronic energy differences were computed using the large ANO-L basis set and the CASSCF/BS1 optimized geometries. The CASSCF/BS1 harmonic vibrational frequencies were used to evaluate the ZPVE, except for the 1^1A_2 state since the C_{2v} optimized structure corresponds to a transition state. In all cases, the ZPVE difference is around -0.02 eV. As a way of reflecting the electronic structure changes, Table 5 also includes the dipole moment, μ, computed at the CASSCF level for each of the states.

3 is a carbene with a singlet ground state [1, 6, 11, 15]. The CASSCF wave function is dominated by the $...(2b_2)^2(7a_1)^2(1b_1)^2$ electronic configuration with a weight of 85%. The σ lone-pair orbital at the carbene center, C_1 (Fig. 1), is related to the $7a_1$ orbital; the $2b_2$ and $1b_1$ orbitals describe the two perpendicular C—C bonds of π type, with the $2b_2$ orbital in the molecular plane and connecting the C_1 and C_2 atoms. As can be seen in Table 4, the lengths of the two C—C double bonds are slightly different. The difference between the two bond lengths increases when the basis set is extended (from 0.019 Åwith the BS1 basis set to 0.054 Å with the BS2 basis set), which also improves the agreement with the CCSD(T) values reported by Sherrill et al. [16]. The shorter C_1—C_2 bond compared to the C_2—C_3 bond

Table 4. Bond lengths (Å) and angles (°) for the ground and lowest excited states of propadienylidene, **3**, compared to other ab initio results. Atom numbering according to Fig. 1

Method	C_1—C_2	C_2—C_3	C_3—H	H—C_3—H
1^1A_1 Ground state				
CASSCF/BS1	1.317	1.336	1.111	117.1
CASSCF/BS2	1.289	1.343	1.098	117.1
CCSD(T)/TZ(2df,2pd)[a]	1.293	1.333	1.085	117.3
B3LYP/6-311G(d,p)[b]	1.285	1.323	1.089	116.6
1^3B_1 state				
CASSCF/BS1	1.257	1.380	1.105	118.7
CASSCF/BS2	1.247	1.371	1.093	118.7
CCSD(T)/TZP[c]	1.238	1.369	1.081	119.0
1^3A_2 state				
CASSCF/BS1	1.345	1.366	1.106	119.6
1^1A_2 state				
CASSCF/BS1[d]	1.340	1.386	1.107	119.2
CASSCF/6-311G(d,p)[b]	1.307	1.390	1.073	120.0
1^1B_1 state				
CASSCF/BS1	1.232	1.447	1.102	119.8
CASSCF/6-311G(d,p)[b]	1.208	1.443	1.071	120.2

[a] Ref. [16]
[b] Ref. [17]
[c] Ref. [8]
[d] Structure corresponding to a transition state (one imaginary frequency of b_2 symmetry)

Table 5. Adiabatic excitation energies (eV) for the lowest excited states of **3** compared to other ab initio results. All calculations at the CASSCF/BS1 optimized geometries

State	CASPT2	μ[a](D)	CC[b]	MRCI[c]	Expt.
1^1A_1	0.0	3.86			
1^3B_1	1.16	0.82			1.29[d]
1^3A_2	1.49	3.44			
1^1A_2	1.69[e]	3.29	1.85	1.77	<1.73[f]
1^1B_1	1.93	1.10	2.52	2.05	2.32 + 0.01[f]

[a] Dipole moment computed at the CASSCF level with the BSL basis set
[b] EOMEE-CCSD results obtained with the cc-pVQZ basis set. ZPE energies included. Ref. [19]
[c] Ref. [17]. MRCI + D results obtained with an ANO (4s3p2d for C, 3s2p for H) basis set
[d] Photoelectron spectrum of propadienylidene anion [32]
[e] Not the exact adiabatic excitation energy since the C_{2v} structure is a saddle point
[f] Electronic absorption spectrum [19]

(1.289 versus 1.343 Å at the CASSCF/BS2 level) indicates that some of the π_x electron density is shifted towards the vacant out-of-plane p_x orbital at the carbene center. The electronic configuration which describes this feature of the electronic structure appears with a weight of 4% in the CASSCF wave function. The σ lone-pair orbital and the shifting of the π_x electron density towards the carbene center explain the large dipole moment of 3.86 D.

From the photoelectron spectrum of the propadienylidene anion, Robinson et al. [32] determined the singlet–triplet splitting of **3** to be 29.7 ± 0.2 kcal/mol. As can be seen in Table 5, the 1^3B_1 state is the lowest triplet state of **3**. The computed value for the adiabatic excitation energy to this state is 26.8 kcal/mol (1.16 eV), slightly below the experimental value [32]. Regarding the geometry, the results collected in Table 4 show that the C_1—C_2 bond length is shortened, while the C_2—C_3 bond length increases in comparison with the ground-state structure. It should also be noted that the CASSCF/BS2 optimal bond lengths for the 1^3B_1 state deviate by less than 0.01 Å from the CCSD(T)/triple-zeta polarization (TZP) values reported by Ochsenfeld et al. [8].

The next excited states are the triplet and singlet states of A_2 symmetry which arise from the one-electron promotion $2b_2 \rightarrow 2b_1$; the $2b_1$ orbital corresponds to the π orbital at the carbene center, which is partially delocalized over the carbon holding the two hydrogen atoms (Fig. 1). The triplet and singlet A_2 states are predicted to have similar C_{2v} geometries with longer C—C bonds than in the ground state (Table 4), as a result of the removal of one electron from a bonding orbital. The harmonic vibrational analysis revealed, however, that the CASSCF/BS1 optimized geometry for the 1^1A_2 state has one imaginary frequency corresponding to the in-plane C—C—C bending mode. Jackson et al. [20] also optimized, within C_{2v} symmetry, the geometry of the 1^1A_2 state at the CASSCF level, but used a smaller active space (six electrons in nine orbitals). According to these authors, the C_{2v} structure of the 1^1A_2 state, which is included in Table 4 for the sake of comparison, has no imaginary frequencies at either the CASSCF or the CIS levels of theory [20]. A C_{2v} geometry has been predicted for the 1^1A_2 state using the equation-of-motion coupled-cluster method in the singles and doubles approximation (EOMEE-CCSD), although the optimized geometry and harmonic vibrational frequencies have not been reported [19].

The adiabatic excitation energy to the 1^3A_2 state is computed to be 1.49 eV. As can be seen in Table 5, the 1^1A_2 state is predicted to appear close in energy, at 1.69 eV. This result does not, however, represent a truly adiabatic excitation energy since one imaginary frequency was found for the 1^1A_2 structure. Considering that the $1^1A_1 \rightarrow 1^1A_2$ transition is symmetry-forbidden and the value estimated for the energy, it is feasible to assign the 1^1A_2 state to the weak features observed at energies lower than 1.73 eV in the electronic absorption spectrum of **3** [19]. The same assignment has been suggested by Stanton et al. [19] on the basis of their EOMEE-CCSD results.

The next excited state is the 1^1B_1 state related to the one-electron promotion $7a_1 \rightarrow 2b_1$, which appears with a weight of 89% in the CASSCF wave function. As the results collected in Table 4 show, the C—C bond lengths in the 1^1B_1 state change considerably compared to the ground-state values. Thus, the C_1—C_2 length decreases and the C_2—C_3 length increases in such a way that they become close to triple and single bonds, respectively. The CASSCF geometry reported by Jackson et al. [20] yields an even shorter C_1—C_2 bond (1.208 Å).

The transition from the ground state to the 1^1B_1 state is optically allowed and has an adiabatic excitation energy of 1.93 eV according to the present results. A band showing a well-resolved vibrational structure has been observed in the visible region of the spectrum (535–382 nm) of **3**, with the 0–0 transition located at 535 nm (2.32 eV) [19]. The 1^1B_1 state contributes then to the band detected in the visible region. As regards the other theoretical results included in Table 5, it is noted that the EOMEE-CCSD energies [19] are always larger than the CASPT2 results. Thus, both sets of excitation energies deviate from the experimental data in opposite directions. The MRCI values reported by Mebel and coworkers [17, 20] are closer to the present results. They were obtained using a CASSCF wave function (eight electrons distributed in ten orbitals) as a reference for the MRCI treatment and the Davidson correction for quadruple excitations.

3.3 Propargylene

The C_3H_2 isomer with the H—C—C—C—H connectivity is commonly known as propargylene and has a triplet ground state [5]. As stated in the introduction, a 1,3-diradical form, with two identical C—C bonds and a bent carbene structure with one short and one long C—C bond (acetylenic structure) has usually been assumed to be the equilibrium geometry. We performed geometry optimizations at the CASSCF level within the constraints of the C_2 and C_s symmetry groups, respectively. In each symmetry, the triplet ground state, the corresponding singlet state, and the closed-shell singlet state

were studied. The CASSCF optimized geometries are collected in Table 6 for C_2 **2** and in Table 7 for C_s **2**. For the sake of comparison, these tables also include the optimal bond lengths and angles determined at the CCSD(T) level [8, 14, 33], as well as density functional results when available [17].

The C_2 and C_s structures of the triplet ground state of **2** are predicted to be nearly degenerate, differing by only 0.16 kcal/mol at the CASPT2/BSL level in favor of the C_2 geometry. In addition, both the C_2 and the C_s structures are characterized as minima according to the CASSCF harmonic vibrational frequencies. The C_2 and C_s forms of **2** have previously not been characterized simultaneously as minima at any level of theory [7, 8]. The C_s carbene structure has only been found to be an equilibrium geometry for **2** at the second-order Møller–Plesset (MP2) and fourth-order Møller–Plesset (MP4) levels, and this was considered as an artifact of the Møller–Plesset treatment [7].

An extensive investigation of the triplet C_3H_2 isomers was recently performed by Ochsenfeld et al. [8] using the coupled-cluster method [CCSD(T) level]. These CCSD(T) calculations place the optimal C_s structure of **2** less than 0.2 kcal/mol above the C_2 equilibrium geometry, in agreement with the present CASPT2 results. The C_s structure is, however, characterized as a saddle point with one imaginary frequency at the CCSD(T) level [8]. In addition to the C_s transition state, Ochsenfeld et al. [8] reported two higher-order saddle points corresponding to geometries of **2** of C_{2v} and $D_{\infty h}$ symmetries, which were predicted to lie 0.9 kcal/mol above the C_2 minimum. Thus, the CCSD(T) results indicate that the triplet C_3H_2 potential-energy surface is extremely shallow in the vicinity of the most stable C_2 geometry of **2** [8]. This shallowness is also illustrated by the small energy difference computed between the C_2 and C_s forms of **2**. Herges and Mebel [7] obtained, however, a larger energy difference between the two geometries by means of extrapolation of computed MR-CI energies to full CI values. The results were, however, found to be very dependent on the basis set used. Thus, the C_2 diradical structure was predicted to be the most stable only when the largest basis set, 6-311G(2d,2p), was used, with the C_s carbene structure 5.8 kcal/mol higher in energy (full CI extrapolated values). On the basis of this theoretical result and the better agreement of the harmonic vibrational frequencies computed for the C_2 structure with the experimental IR spectrum, the

Table 6. Bond lengths (Å) and angles (°) for the ground and lowest excited states of C_2 propargylene, **2**, compared to other ab initio results. Atom numbering according to Fig. 1. The relative energies with respect to the ground state and the multiconfigurational second-order perturbation (*CASPT2*) total energy of the ground state are also included

Method	C_1—C_2	C_2—H	C_2—C_1—C_2	C_1—C_2—H	C_2—C_1—C_2—H
1^3B ground state (−115.080172 au)					
CASSCF/BS1	1.294	1.092	166.0	151.0	147.0
CASSCF/BS2	1.284	1.079	167.9	151.7	143.9
CCSD(T)/TZP[a]	1.279	1.067	171.9	156.5	
CCSD(T)/cc-pVTZ[b]	1.273	1.060	174	162	143
B3LYP/6-311G(d,p)[c]	1.269	1.063	177.5	171.4	135.3
1^1A state (14.1 kcal/mol)					
CASSCF/BS1	1.316	1.109	155.3	124.1	180.0
CASSCF/BS2	1.305	1.094	156.6	125.0	180.0
QCISD/6-31G*[d]	1.302	1.086	162.0	126.9	
CCSD(T)/cc-pVTZ[e]	1.293		162.4		
1^1B state (21.5 kcal/mol)					
CASSCF/BS1	1.284	1.087	170.7	162.0	156.0

[a] Ref. [8]. A value of 88° was obtained for the H—C—C—H torsion angle
[b] Ref. [14]
[c] Ref. [17]
[d] Ref. [7]
[e] C_{2v} structure from Ref. [33]

Table 7. Bond lengths (Å) and angles (°) for the ground and lowest excited states of C_s **2** compared to other ab initio results. Atom numbering according to Fig. 1. The relative energies with respect to the ground state and the CASPT2 total energy of the ground state are also included

Method	C_1—C_2	C_1—C_3	C_2—H_1	C_3—H_2	C_2—C_1—C_3	C_1—C_2—H_1	C_1—C_3—H_2
1^3A″ ground state (−115.079915 au)							
CASSCF/BS1	1.264	1.334	1.088	1.096	172.9	177.5	139.9
CASSCF/BS2	1.255	1.325	1.074	1.083	173.9	178.2	140.0
CCSD(T)[a]	1.262	1.296	1.064	1.069	172.6	173.4	150.9
1^1A′ state (14.2 kcal/mol)							
CASSCF/BS1	1.244	1.399	1.088	1.129	173.6	179.2	107.8
CASSCF/BS2	1.235	1.388	1.074	1.113	173.8	179.5	108.7
CCSD(T)[b]	1.237	1.357			168.9		
1^1A″ state (20.7 kcal/mol)							
CASSCF/BS1	1.280	1.295	1.086	1.088	175.7	179.6	156.9

[a] TZP basis set [8]
[b] cc-pVTZ basis set [33]

ground state of **2** was concluded to have a C_2 1,3-diradical structure [7, 9]. The present results, as well as the CCSD(T) investigation performed by Ochsenfeld et al. [8], suggest, however, a nonrigid structure for **2**, which makes the harmonic vibrational approximation less reliable.

The C_2 geometry of the ground state (1^3B state) of **2** is related to a 1,3-diradical electronic structure, with a double bond connecting the carbon atoms and an almost linear carbon skeleton, as reflected by the optimized geometries included in Table 6 and illustrated in Fig. 1. The computed spin densities support this description, having the values +1.2 (C_2) and −0.3 (C_1) at the CASSCF/BS1 level. The results collected in Table 6 show that the C—C bond lengths deviate less than 0.01 Å from the CCSD(T) values, as noted for the other C_3H_2 isomers. The differences in the bond angles are, however, larger, between 6 and 10° when the results are compared to the CCSD(T) values obtained with the correlation-consistent polarized valence triple-zeta (cc-pVTZ) basis set of Dunning [14]. The CASSCF/BS2 bond angles differ less (4–5°) from the the CCSD(T) results [8] (Table 6). The computed values for the bond angles are sensitive to the basis set used in the optimization process, in particular to the inclusion of functions with high angular momentum. The optimized geometry at the B3LYP level reported by Mebel et al. [17] shows significant differences with respect to the CASSCF and CCSD(T) geometries concerning mainly the bond angles, as can be seen in Table 6. A value of 155° has been estimated for the C—C—H bond angle from the EPR spectrum [9], which is in agreement with the CASSCF and CCSD(T) results [14] [151.7 and 162° at the CASSCF/BS2 and CCSD(T)/cc-pVTZ levels, respectively].

As can be seen in Table 7, the planar C_s geometry optimized for the ground state ($1^3A''$ state) of **2** differs significantly from the acetylenic carbene structure, with one single and one triple C—C bond, drawn in Fig. 1. The most important discrepancy is found for the C_1—C_3 bond length (1.325 Å at the CASSCF/BS2 level), which is better described as a double bond than as a single bond. Ochsenfeld et al. [8] obtained an even shorter C_1—C_3 bond length, 1.296 Å at the CCSD(T)/TZP level. The C_1—C_2 bond is somewhat elongated compared to a triple bond. The C_s structure is predicted to be almost linear, except for the hydrogen atom bound to the carbene center (H_2 atom). Thus, the C_1—C_3—H_2 bond angle is computed to be 140.0° at the CASSCF/BS2 level, around 10° smaller than the value determined by Ochsenfeld et al. [8] using the CCSD(T) method.

The $1^3A''$ ground state of C_s **2** is mainly described by the one-electron promotion from the σ lone-pair orbital at the carbene center to the carbene out-of-plane (p_z) orbital. The p_z orbital at the carbene center is delocalized towards the other terminal carbon atom (C_2), a characteristic reflected in the spin densities computed for the $1^3A''$ state. The values +0.8 (C_2), −0.3 (C_1), and +1.5 (C_3) were obtained for the spin densities at the CASSCF level, indicating that there is a certain shifting of the electron density away from the carbene center (C_3 atom). These electronic features, together with the geometric distortions with respect to the acetylenic carbene structure reported here, suggest an important contribution of a 1,3-diradical structure to the $1^3A''$ state. The C_s structure of the ground state of **2** is therefore closely related to the C_2 structure, which is predicted to be almost isoenergetic. As stated earlier, a nonrigid geometry is proposed for **2**, with the C_2 and C_s forms connected through the molecular vibrations. The information derived from the IR spectrum will be analyzed when discussing the computed harmonic vibrational frequencies.

The two optimized structures of the closed-shell singlet state are almost degenerate, similar to the results obtained for the triplet ground state. The results collected in Table 7 show that the C_s structure of **2** is a good representation for the $1^1A'$ state. The values 1.235 and 1.388 Å are predicted for the triple- and single-bond lengths, respectively, at the CASSCF/BS2 level, indicating a shift of the electron density from the triple bond towards the vacant p_z orbital at the carbene center. As expected, the C_1—C_3—H_2 bond angle is considerable reduced compared to its value in the triplet state (108.7 versus 140.0° at the CASSCF/BS2 level) owing to the double occupancy of the σ lone-pair orbital in the $1^1A'$ state. According to the CASSCF harmonic vibrational frequencies, the C_s carbene structure of **2** is a minimum on the singlet C_3H_2 energy surface, in agreement with the characterization obtained at other levels of theory [7, 33].

The optimization process within the C_2 symmetry restrictions for the closed-shell singlet state led to a more symmetric C_{2v} structure. One imaginary frequency was found, however. This structure is thus characterized as a transition state connecting the two equivalent C_s structures, in accordance with the results recently obtained by Stanton et al. [33] using the coupled-cluster methods. They computed an energy difference of 0.51 kcal/mol between the C_s and C_{2v} structures with the CCSD(T) method and a cc-pVTZ basis set [33]. The energy difference is reduced by means of the inclusion of triple excitations [33]. The CASPT2 calculations locate the C_s equilibrium geometry 0.21 kcal/mol above the C_{2v} structure. The use of CASSCF optimized geometries together with the quite small energy difference explain the reverse order of stability (the C_{2v} transition state lower in energy) determined at the CASPT2 level.

The lowest singlet excited state of **2** was exhaustively investigated by Herges and Mebel [7] at different levels of theory. According to their HF, MP2, and MP4 calculations, singlet **2** was also predicted to be a carbene with C_s symmetry that undergoes a fast automerization via a C_{2v} transition state. Single-point calculations at higher levels of theory favored, however, the C_{2v} structure, which was found to be a minimum at the QCISD(T)/6-31G** level, while the C_s structure could not be characterized as a stationary point. Thus, Herges and Mebel [7] proposed a C_{2v} structure as the equilibrium geometry for singlet **2**, which was estimated to be 2.1 kcal/mol more stable than the C_s form on the basis of extrapolated full CI energies. The B3LYP calculations carried out by Mebel et al. [17] predict two minima of C_{2v} and C_{2h} symmetries for singlet **2**, while a C_s structure is characterized as a transition state but is very close in energy to the C_{2v} form. The recent study performed by

Stanton et al. [33] and the present investigation support, however, a carbene C_s structure for the closed-shell singlet state of **2** and predict the C_{2v} structure to be almost degenerate but to correspond to a transition state. The singlet–triplet splitting is estimated to be around 14 kcal/mol (14.3 is the energy difference between the 1^3B and $1^1A'$ states) at the CASPT2/BSL level, to be compared with the value 11.9 kcal/mol determined at the CCSD(T)/cc-pVTZ by Stanton et al. [33].

The next excited state is the open-shell singlet. Both C_2 and C_s geometries are characterized as minima according to the CASSCF harmonic vibrational frequencies. The CASPT2 calculations locate the C_s structure ($1^1A''$ state) only 0.6 kcal/mol lower than the C_2 geometry, suggesting again a quite flat surface. The energy difference with respect to the corresponding triplet ground state is computed to be 21.5 kcal/mol (C_2 symmetry) and 20.7 kcal/mol (C_s symmetry), respectively. The C_2 structure (1^1B state) is almost linear, with larger bond angles compared to the 1^3B state. In the C_s structure, the C—C bond lengths become close to each other and can be described as double bonds, in line with the results reported by Mebel et al. [17]. These authors studied the singlet and triplet excited states of **2**, also performing geometry optimizations at the CASSCF level and using the CIS approach to characterize the structures. They computed vertical and adiabatic excitation energies by means of the MRCI method using as a reference a CASSCF wave function and with the Davidson correction for quadruple excitations. A value of 8.5 kcal/mol was obtained for the adiabatic excitation energy of the $1^1A' \rightarrow 1^1A''$ transition using an ANO basis set similar to our BS2 basis set. A somewhat smaller energy difference, 6.5 kcal/mol, is predicted here, on the basis of the CASPT2 calculations at the CASSCF/BS1 optimized geometries for the C_s symmetry singlet states.

3.4 Cyclopropyne

The smallest cyclic alkyne **4**, has been characterized as a high-lying saddle point on the singlet C_3H_2 energy surface [6, 14, 16, 34]. One or two imaginary vibrational frequencies have been found for **4** depending on the level of theory used in the calculations [14, 16]. This isomer has been predicted to lie 58–61 kcal/mol higher in energy than the global minimum **1** using the CCSD(T) method [14, 16]. However, Seburg et al. [14] have recently reported results from calculations at different levels of theory which predict a structure with a planar tetracoordinate carbon (**4a** in Fig. 1) 7–10 kcal/mol lower in energy than the expected structure for **4** with the tetrahedral carbon atom (**4b** in Fig. 1). The present study considers both structures: the planar form (**4a**) and the one with the tetrahedral carbon, which will be denoted as the perpendicular structure (**4b**). Only the singlet ground state and the lowest triplet state will be studied.

The CASSCF optimized geometries are presented in Table 8, along with the CCSD(T) structural parameters reported by Seburg et al. [14] and the CISD values obtained by Sherrill et al. [16] for the 1^3B_2 state of **4b**.

Table 8. Bond lengths (Å) and angles (°) for the ground and lowest triplet states of cyclopropyne, **4**, compared to other ab initio results. Atom numbering according to Fig. 1

Method	C_1—C_2	C_2—C_2	C_1—H	C_2—C_1—C_2	H—C_1—H
Planar conformation					
1^1A_1 ground state					
CASSCF/BS1	1.590	1.353	1.094	50.4	110.5
CASSCF/BS2	1.582	1.340	1.081	50.1	110.9
CCSD(T)[a]	1.544	1.331	1.084	51	112
Perpendicular conformation[b]					
1^1A_1 ground state					
CASSCF/BS1	1.558	1.279	1.096	48.5	113.2
CASSCF/BS2	1.548	1.265	1.082	48.2	113.5
CCSD(T)[a]	1.527	1.249	1.085	48	114
1^3B_2 state					
CASSCF/BS1	1.592	1.327	1.092	49.3	115.3
CASSCF/BS2	1.586	1.314	1.080	48.9	115.7
CISD/DZP[c]	1.556	1.300	1.089	49.4	115.4

[a] cc-pVTZ basis set [14]
[b] Structure with a tetrahedral carbon atom (C_1 atom)
[c] Ref. [16]

The present geometry optimizations were performed within the constraints of C_{2v} symmetry. From the results collected in Table 8, significant differences can be deduced between **4a** and **4b**. **4a** is better described as having a double C_2—C_2 bond and weak C_1—C_2 single bonds, as indicated by the computed bond distances (1.340 and 1.582 Å, respectively, at the CASSCF/BS2 level). **4b** contains, however, a weak C_2—C_2 triple bond (1.265 Å) and C_1—C_2 single bonds (1.548 Å). A difference of around 2° is found between the C_2—C_1—C_2 bond angles of both structures, indicating quite similar ring strain. The same trends are noted when comparing the CCSD(T) optimized geometries reported by Seburg et al. [14]. The most important difference between the CASSCF/BS2 and CCSD(T) optimized geometries is found for the C_1—C_2 bond length of **4a**, which is around 0.04 Å larger at the CASSCF level, as shown in Table 8.

A comparison of the optimized geometries for **4a** and **4b** suggests that these two structures are not simply related by the twist of the CH_2 group. An analysis of the CASSCF wave functions can provide more insight into this point. Thus, **4a** is mainly described by the $...(5a_1)^2(3b_2)^2(6a_1)^2(1b_1)^2$ electronic configuration, which appears with a weight of 89% in the CASSCF wave function. Here, the $1b_1$ orbital is a delocalized π orbital, the $6a_1$ orbital corresponds to a σ orbital with antibonding character between the C_1 and C_2 atoms, and the $3b_2$ orbital is related to a lone-pair orbital located on the equivalent C_2 atoms. The best way of describing **4a** seems to result from the interaction of methylene (CH_2) and C=C. As indicated by the structural parameters (Table 8), **4a** is not a good representation of the optimized geometry for planar **4** since a double C—C bond is maintained. In contrast, perpendicular **4** is quite well represented by structure **4b** depicted in Fig. 1, showing a triple C—C bond. On the other hand, **4b** has been found to be the C_3H_2 isomer with the largest multiconfigurational character.

Although the CASSCF wave function is dominated by the $...(5a_1)^2(2b_2)^2(2b_1)^2(6a_1)^2$ electronic configuration with a weight of 83%, a second important configuration related to the two-electron promotion $(6a_1)^2 \rightarrow (3b_2)^2$ appears having a weight of 5%. The contribution of this second configuration has also been shown in previous theoretical studies [16, 34]. It can be rationalized by the fact that the $3b_2$ orbital is very low in energy, which is also reflected in a very low lying triplet state for **4b**.

The present study also finds **4a** to be more stable than **4b**, in agreement with the theoretical results reported by Seburg et al. [14]. The energy difference is computed to be 4.6 kcal/mol (CASPT2/BSL result), which should be compared to the value 7.5 kcal/mol obtained at the CCSD(T)/cc-pVTZ level by Seburg et al. [14]. It seems to be fortuitous that the two structures are quite close in energy, considering the differences found in their molecular and electronic structures.

According to the CASSCF harmonic vibrational frequencies, **4b** is a transition state. The imaginary frequency is the b_2 asymmetric C—C stretch (ring-opening) mode. Seburg et al. [14] have, however, predicted the vibrational frequency of the methylene twist mode (a_2 symmetry) to be also imaginary for this structure using different levels of theory, such as CCSD(T)/cc-pVTZ, QCISD/6-31G*, and B3LYP/6-31G*. This different result compared to CASSCF can be attributed to the lack of the doubly excited $(6a_1)^2 \rightarrow (3b_2)^2$ electronic configuration in the reference function used with the previously mentioned methods, which is not compensated by the extensive treatment of the electron correlation performed, for instance, at the CCSD(T) level. A previous study performed by Sherrill et al. [16] showed that the vibrational frequency for the a_2 methylene twist mode becomes real when the doubly excited $(6a_1)^2 \rightarrow (3b_2)^2$ electronic configuration is included in the reference wave function via the two-configuration (TC) SCF and TC-CISD methods. In contrast, single-reference techniques yielded an imaginary value for the a_2 mode, as well as for the b_2 mode, of **4b** [16].

On basis of the TC-CISD results, Sherrill et al. [16] suggested that **4b** could be the transition state in the automerization of **3** since the b_2 imaginary mode leads to ring opening towards **3** . The automerization of **3** implies the interchange of the C_1 and C_2 atoms (Fig. 1), those not bound to hydrogen atoms, and has been experimentally detected under photolysis with $\lambda > 444$ nm (<64 kcal/mol) [14, 35]. The CASSCF vibrational analysis supports the characterization of **4b** as a transition state in the automerization of **3**. The CASPT2 calculations locate **4b** 44.6 kcal/mol above **3**, indicating that this transition state is accessible under the experimental conditions (below 64 kcal/mol) [14, 35].

4a is computed to lie 40.0 kcal/mol above **3** and, therefore, it is also accessible experimentally. Actually, Seburg et al. [14] have proposed **4a** as the transition state in the automerization of **3** on the basis of the vibrational analysis and its lower energy in comparison with **4b**. The planar isomer was computed to lie 39.2 kcal/mol above **3** at the CCSD(T)/cc-pVTZ level of theory; thus, within the experimental range. **4b** was predicted to have two imaginary vibrational frequencies (methylene twist and ring-opening modes), while only the b_2 ring-opening mode was found to be imaginary for **4a** according to their theoretical results [14]. **4a** is here also computed to have one imaginary vibrational frequency related to a mode of b_2 symmetry; however, this imaginary b_2 mode corresponds mainly to an in-plane asymmetric hydrogen movement, with some mixing from the ring opening. On the basis of the type of imaginary mode determined in the present study, **4a** cannot be considered as the transition state in the automerization process of **3**, even if the computed energy difference with respect to **3** is consistent with the experimental conditions for the process [14, 35].

The results of the CASSCF vibrational analysis performed here suggest that **4a** could be the transition state in the conversion of **3** to **1**. This isomerization process has also been detected under photolysis with $\lambda > 444$ nm but at longer times, suggesting a 1,2-hydrogen migration [14].

As previously stated, the present results show that **4a** and **4b** differ not only in the CH_2 twist angle but also in the type of multiple bond. Indeed, only **4b**, with a triple C—C bond, should be called cyclopropyne. A comparison of the CASSCF vibrational frequencies, with a b_2 imaginary mode in both structures, gives additional support to the reported differences.

The lowest triplet state of **4b**, 1^3B_2 state, is computed at 9.3 kcal/mol above the singlet ground state, in agreement with the value of 9.2 kcal/mol predicted by Sherrill et al. [16] using the CCSD(T) method. Theoretical studies at different levels of theory agree in the small singlet–triplet splitting in this isomer [6, 16, 34]. The 1^3B_2 state has been characterized as a minimum on the basis of the HF harmonic vibrational frequencies [6, 16, 34], a result which is confirmed by the present CASSCF computed frequencies. The 1^3B_2 state is mainly described by the one-electron promotion $6a_1 \rightarrow 3b_2$. The antibonding character of the $3b_2$ orbital with respect to the C—C bonds accounts for the lengthening found in these bonds in comparison with the ground state, as can be deduced from the results collected in Table 8. Thus, the triple bond becomes a double bond in the 1^3B_2 state, with an optimal bond length of 1.314 Å at the CASSCF/BS2 level. The stability of the triplet state has been attributed to this change in the bond order [34].

As regards **4a**, the 1^3B_1 state is predicted to be the lowest triplet state, appearing 45.1 kcal/mol above the corresponding ground state. The optimal values determined for the C_1—C_2 and C_2—C_2 bond lengths are 1.793 and 1.312 Å, respectively, at the CASSCF/BS1 level. Therefore, the 1^3B_1 state in **4a** seems to correspond to a weakly interacting methylene and C=C fragments. Three imaginary frequencies are found for this structure.

3.5 Propenediylidene

Two divalent carbon centers are found in the C_3H_2 isomer **5**, as illustrated in Fig. 1; this isomer is, therefore, expected to be quite high in energy. The cis and trans forms with respect to the positions of the hydrogen atoms were studied. The geometries were fully optimized within

the C_s symmetry restrictions. All the geometry optimizations performed here for the singlet states of both the cis and trans forms of **5** led to **1**, that is the global minimum of the singlet C_3H_2 energy surface, as reported in previous theoretical studies [14, 15]. The present calculations predict, however, stable structures, corresponding to local minima, for the triplet states of the cis and trans geometries, which were found to be nearly degenerate. According to our CASPT2/BSL results the trans form of **5** is only 0.6 kcal/mol more stable than the cis structure. Ochsenfeld et al. [8] have characterized the trans form of **5** as the highest minimum on the triplet C_3H_2 energy surface, appearing at 58 kcal/mol above the global triplet minimum (C_2 **2**) according to their CCSD(T)/TZP calculations. A similar value, 60 kcal/mol, is found here for the energy difference between the trans form of **5** and C_2 **2**. Although Ochsenfeld et al. [8] were unable to locate a stationary point corresponding to the cis form of **5**, they did not rule out its possible existence and attributed this result to a very flat energy surface around the cis isomer of **5**. Seburg et al. [14] reported that both triplet **5** isomers are nearly degenerate minima, in agreement with the present results.

For the two isomers, cis and trans, the triplet state is mainly described by the electronic configuration with one electron in the σ lone-pair orbital at the carbene center holding the hydrogen atom (C_3, Fig. 1) and the other electron in the corresponding out-of-plane π orbital, which is partially delocalized over the other carbene atom of the molecule (C_1). The C—C bond lengths deviate somewhat from the values expected for double (C_1—C_2) and single (C_2—C_3) bonds, illustrating the electron delocalization in both structures. For instance, the values 1.350 and 1.419 Å are predicted for the C_1—C_2 and C_2—C_3 bond lengths, respectively, in the cis form of **5** at the CASSCF/BS1 level of theory. Geometry optimizations and vibrational frequency calculations were not carried out with the larger BS2 basis set since **5** represents a high-lying structure in the triplet C_3H_2 energy surface. In addition, previous experience with the other isomers shows that the results concerning the type of stationary point are not affected by the extension of the basis set.

3.6 Relative energies of C_3H_2 isomers

The relative energies of C_3H_2 isomers are discussed in this section and are compared with previous theoretical results. Table 9 collects the relative energies for the lowest singlet and triplet states of each isomer determined at the CASPT2 level of theory, using the BSL basis set and CASSCF/BS1 optimized geometries. The values corrected by the ZPVE differences are also presented in the table. Harmonic vibrational frequencies obtained at the CASSCF/BS2 level were used to compute the ZPVE in the structures characterized as minima, except for the cis and trans forms of **5** for which the vibrational frequencies were calculated only with the smaller BS1 basis set. The number of imaginary frequencies found for each structure is also listed in Table 9. The results collected in Table 9 show that the relative energies of C_3H_2 isomers are always reduced when the ZPVE differences are taken into account.

Table 9. Number of imaginary frequencies, Zero-point vibrational energies (*ZPVE*, kcal/mol), and CASPT2 relative energies (kcal/mol) for singlet and triplet C_3H_2 isomers

C_3H_2 isomer[a]	Imag. Freq.	ZPVE[b]	ΔE^{c}_{CASPT2}	ΔE^{d}
1s cyclic	0	20.1	0.0	0.0
2t C_2 HCCCH	0	15.8	9.2	4.9
2t C_s HCCCH	0	16.5	9.4	5.8
3s H_2CCC	0	18.9	10.7	9.5
2s C_{2v} HCCCH	1		23.3	
2s C_s HCCCH	0	17.5	23.6	21.0
3t H_2CCC	0	18.6	38.0	36.5
1t asym. cyclic	0	18.8	49.5	48.2
1t cyclic	2		54.6	
4s planar	1		50.7	
4s perpendicular	1		55.4	
4t perpendicular	0	20.0	64.7	64.6
5t trans HCHCC	0	e	69.1	
5t cis HCHCC	0	e	69.7	

[a] See Fig. 1. **s** and **t** stand for the singlet and triplet states, respectively
[b] Values obtained using the CASSCF/BS2 harmonic vibrational frequencies
[c] CASPT2 single-point calculations at the CASSCF/BS1 optimized geometries
[d] ΔE includes the ZPVE differences computed at the CASSCF/BS2 level [$\Delta E = \Delta E_{CASPT2} + \Delta(ZPVE)$]
[e] Only the CASSCF/BS1 harmonic vibrational frequencies are available

As can be seen in Table 9, **2t** is predicted to be more stable than **3s**, in agreement with the results reported by Seburg et al. [14] at various levels of theory. According to the present results, these two isomers, **2t** and **3s**, appear at energies lower than 11 kcal/mol with respect to the most stable C_3H_2 isomer. Furthermore, the relative energies are considerably decreased for **2t** when the ZPVE differences are added, although these values should be taken with some caution. As stated earlier, the nonrigid geometry predicted for **2t** makes the validity of the harmonic approximation questionable.

The relative energies of C_3H_2 isomers on the singlet and triplet energy surfaces are presented in Tables 10 and 11, respectively, including comparison with other ab initio results. The energy difference between **2t**, the most stable isomer on the triplet C_3H_2 energy surface, and **1s** determined at various levels of theory is reported in Table 12. According to our results, the C_2 and C_s structures are stable for **2t**, differing only by 0.2 kcal/mol (electronic energy difference) (Table 9). All values included in Table 12 correspond to C_2 **2t**. Jonas et al. [6] also considered the C_s structure of **2t**, which is predicted to lie 0.7 kcal/mol above the C_2 form on the basis of their spin-projected MP4 calculations with the 6-311G(2df) basis set, in line with the present results.

As can be seen in Table 12, the electronic energy difference between the most stable triplet and singlet C_3H_2 isomers varies between 6.4 and 14.0 kcal/mol depending on the level of theory used in the calculations [6, 14]. Comparing the CASPT2 result, 9.2 kcal/mol, to the other theoretical values listed in Table 12, the largest

Table 10. Computed relative energies (kcal/mol) of singlet C_3H_2 isomers. Values within *parentheses* include the ZPVE differences

C_3H_2 isomer[a]	This work CASPT2	Jonas et al. [6] MP4[b]	Seburg et al. [14][c]	
			CCSD(T)	BLYP
1 cyclic	0.0	0.0	0.0	0.0
3 H_2CCC	10.7 (9.5)	14.2 (13.5)	14.1 (13.2)	7.5 (7.0)
2 C_2 HCCCH	23.3		26.4[d]	
2 C_s HCCCH	23.6 (21.0)	26.6 (24.2)	25.9[d]	
4 planar	50.7		53.2 (50.7)	48.8 (46.6)
4 perpendicular	55.4	61.5 (59.8)	60.7	58.6 (57.2)

[a] See Fig. 1
[b] Results obtained using a 6-311G(2df) basis set and geometries optimized at MP2/6-31G(d) level. Scaled HF/6-31G(d) ZPVE from Ref. [6]
[c] The basis sets used are cc-pVTZ for the CCSD(T) calculations and 6-31G* for the BLYP calculations
[d] Ref. [33]

Table 11. Relative energies (kcal/mol) of triplet C_3H_2 isomers

C_3H_2 isomer[a]	This work		Ochsenfeld et al. [8]		
	CASPT2	ΔE[b]	CCSD(T)[c]	ΔE[d]	MP2[c]
2 C_2 HCCCH	0.0		0.0		0.0
2 C_s HCCCH	0.2	0.9	−0.07		−0.6
3 H_2CCC	28.8	31.6	29.7	32.2	29.8
1 asym. cyclic	40.3	43.3	38.5	41.2	24.9
1 C_{2v} cyclic	45.4		44.8		35.7
4 perpendicular	55.5	59.7			
5 trans HCHCC	59.9		59.1	59.9	61.3
5 cis HCHCC	60.5				

[a] See Fig. 1
[b] CASPT2/BSL relative energies combined with CASSCF/BS2 ZPVE
[c] Results obtained using a QZ2P basis set and geometries optimized at the CCSD(T)/TZP level
[d] CCSD(T)/QZ2P relative energies combined with CCSD(T)/TZP ZPVE

Table 12. Computed energy differences (kcal/mol) between triplet **2** (C_2 structure) and singlet **1**

Method	ΔE[a]	ΔE[b]
CASPT2/BSL	9.2	4.9
CCSD(T)/cc-pVTZ[c]	14.0	9.8
BLYP/6-31G*[c]	6.4	3.6
QCISD/6-31G*[c]	7.9	4.2
PMP4/6-311G(2df)[d]	12.9	8.7

[a] Electronic energy difference
[b] $\Delta E = \Delta E + \Delta(\text{ZPVE})$
[c] Ref. [14]
[d] Ref. [6]

deviation occurs with respect to the CCSD(T)/cc-pVTZ result, which is 4.8 kcal/mol higher, while the QCISD/6-31G* energy difference, 7.9 kcal/mol, is closest to the present result. It is also noted that the ZPVE difference computed at the CASSCF level is almost equal to the value determined at the CCSD(T)/cc-pVTZ level [14].

Jonas et al. [6] studied the C_3H_2 isomers using mainly Møller–Plesset theory. The relative energies of singlet C_3H_2 isomers obtained at the highest level of theory used in their study [6], MP4/6-311G(2df) calculations at geometries optimized at the MP2/6-31G(d) level, are collected in Table 10 together with the present results. Table 10 also includes results from CCSD(T) and density functional (BLYP/6-31G*) calculations performed by Seburg et al. [14]. These authors used the cc-pVTZ basis set of Dunning for the CCSD(T) calculations, which were carried out using the geometries optimized at the same level of theory. All results predict the same order of stability (**1s** > **3s** > **2s** > **4s**) and quite similar relative energies. Furthermore, the electronic energy differences computed at the MP4 and CCSD(T) levels of theory differ by less than 1 kcal/mol and are larger than the CASPT2 values. However, the discrepancy with respect to the CASPT2 results is around 3 kcal/mol, except for **4b**, the highest singlet isomer, which is found to lie about 61 kcal/mol above the global minimum, **1**, at the MP4 and CCSD(T) levels of theory (Table 10) compared to the value 55.4 kcal/mol predicted at the CASPT2 level. It may be noted that **4b** has been found to have nonnegligible MC character. On the other hand, the BLYP/6-31G* energy differences for **3** and **4a** are underestimated in comparison with all the other values included in Table 10. The energy difference between **3** and **1** has been estimated on the basis of experiments to be 11.8 kcal/mol, as reported by Seburg et al. [14]. The value predicted here, 9.5 kcal/mol, is slightly smaller, while the CCSD(T) result, 13.2 kcal/mol, is slightly too large.

The triplet C_3H_2 energy surface has been exhaustively studied by Ochsenfeld et al. [8] using the CCSD(T) method and several basis sets. The CCSD(T) relative energies of triplet C_3H_2 isomers computed by these authors with a quadruple-zeta double polarization basis set and using CCSD(T)/TZP optimized geometries are shown in Table 11 along with their MP2 values determined with the same basis set and geometries [8]. **4** was not considered in the investigation performed by Ochsenfeld et al. [8]. They were unable to find a stationary point corresponding to the cis form of **5**, as discussed previously. The triplet state corresponds to the ground state in **2** and the cis and trans form of **5**. The characterization of the triplet isomers provided by the CCSD(T) vibrational frequencies computed by Ochsenfeld et al. [8] agree with the ones obtained here, except for C_s **2**. Our results predict the C_s structure to be a minimum for the triplet ground state, while the CCSD(T) harmonic vibrational frequencies characterize the structure as a transition state [8]. All the remaining triplet isomers correspond to minima, excluding **1** with C_{2v} symmetry, which was found to have two imaginary frequencies (see earlier). An unsymmetrical structure was characterized as the lowest stable triplet state of **1**.

As can be seen in Table 11, the CASPT2 and CCSD(T) results predict the same energy ordering for triplet C_3H_2 isomers. **2** is the global minimum on the triplet surface, followed by **3**, which appears at 28.8 kcal/mol above C_2 **2** according to the CASPT2/BSL result. The unsymmetrical and C_{2v} structures of **1** appear next in energy, at 40.3 and 45.4 kcal/mol, respectively.

4b is predicted to lie at 55.5 kcal/mol and the cis and trans forms of **5** about 60 kcal/mol above **2**. The CASPT2 relative energies of triplet C_3H_2 isomers deviate at most by 2.3 kcal/mol from the CCSD(T) values reported by Ochsenfeld et al. [8]. Except for **3**, the CASPT2 relative energies computed for the triplet isomers with respect to the most stable triplet isomer are larger than the CCSD(T) values, in contrast to the trend found in the singlet surface. As can be deduced from the results collected in Table 11, the ZPVE differences computed on the basis of the CASSCF and CCSD(T) harmonic frequencies are also quite similar. The CASPT2 and CCSD(T) results show that the MP2 relative energies are underestimated for **1** in both the unsymmetrical and the C_{2v} structures. This also leads to a different energy ordering for the triplet C_3H_2 isomers at the MP2 level of theory. Ochsenfeld et al. [8] attributed the too low value predicted for the energy difference between **1** and the most stable triplet isomer to the overestimation of correlation effects often obtained with the MP2 method.

Summarizing, the present CASPT2 results predict the same energy ordering for the C_3H_2 isomers as the CCSD(T) results, in both singlet and triplet energy surfaces. The CASPT2 relative energies are in most cases within 3 kcal/mol of the CCSD(T) values. The largest discrepancies are found for the energy difference between the most stable triplet and singlet isomers (**2** and **1**, respectively) (Table 12) and for the relative energy of the singlet state of **4b** with respect to **1s** [55.4 kcal/mol at the CASPT2/BSL level compared to 60.7 kcal/mol at the CCSD(T)/cc-pVTZ level [14]]. The good agreement found between the CASPT2 and CCSD(T) results is consistent with the fact that the wave function of the lowest singlet and triplet states is usually dominated by one electronic configuration. A weight equal to or larger than 85% was obtained for the main configuration of the CASSCF wave functions for all systems except the singlet ground state of **4b**, for which a lower weight was found.

3.7 Vibrational spectra

In the following, we briefly examine the computed harmonic vibrational frequencies and IR intensities for the C_3H_2 isomers characterized as minima. The calculations were performed at the CASSCF level with the ANO-S C[4s3p2d]/H[3s2p] basis set. Tables 13–15 show the CASSCF vibrational frequencies and IR intensities computed for the ground states of **1**, **3**, and **2**, respectively, in comparison with other ab initio predicted IR spectra and experimental data reported by Seburg et al. [14] in an argon matrix at low temperature. The calculated IR spectra for the lowest triplet states of **1** and **3** are collected in Tables 16 and 17, respectively, and Table 18 includes the results obtained for the lowest singlet state of **2**.

As the results included in Tables 13–17 show, the CASSCF vibrational frequencies are in agreement with the CCSD(T) frequencies reported by Seburg et al. [14] and Ochsenfeld et al. [8]. Thus, the CASSCF frequencies deviate by less than $\pm 100\ cm^{-1}$ from the CCSD(T) values, except for the two modes related to the CH stretching vibrations which present differences a bit larger but at most within $\pm 150\ cm^{-1}$. As a whole, the IR spectra predicted at the CASSCF level are in line with those determined using the CCSD(T) approach [8, 14] and with the experimental data [14]. **2** represents, however, a different case, as we shall discuss later.

Some quite low vibrational frequencies (below $300\ cm^{-1}$) occur for the ground and lowest triplet states of **3** (Tables 14, 17). These frequencies are related to the out-of-plane (b_1) and in-plane (b_2) bending of carbon skeleton modes and are predicted to have a very low intensity. For the ground state of **3**, the most intense feature of the computed IR spectrum corresponds to the CC stretching mode computed at $2019\ cm^{-1}$, in accordance with the experimental data [14]. The CH wagging mode is most intense in the 1^3B_1 state of **3**, with a CASSCF computed frequency of $630\ cm^{-1}$ (Table 17).

2 is predicted to have a nonrigid geometry, a characteristic which limits the validity of the harmonic approximation for the calculation of the vibrational frequencies; however, the computed harmonic vibrational frequencies were used in previous studies [7, 9] for elucidating the structure of **2** by means of a comparison with the observed IR spectrum. From these studies, a C_2

Table 13. CASSCF computed harmonic vibrational frequencies (cm^{-1}) and IR intensities (km/mol, in *parentheses*) for the ground state of **1** compared to other ab initio results and experimental data

Mode	CASSCF[a]	CCSD(T)[b]	Expt.[c]
b_1	784 (18)	800 (20)	783 (54)
a_1	912 (14)	914 (19)	883 (35)
b_2	948 (4)	914 (4)	895 (14)
a_2	983 (0)	998 (0)	
b_2	1177 (6)	1089 (9)	
a_1	1343 (47)	1316 (48)	1278 (100)
a_1	1612 (1)	1635 (<1)	
b_2	3144 (1)	3259 (<1)	
a_1	3182 (<1)	3307 (<1)	

[a] Calculations using the ANO-S C[4s3p2d]/H[3s2p] basis set
[b] cc-pVTZ basis set [14]
[c] Argon matrix, 8 K [14]

Table 14. CASSCF computed harmonic vibrational frequencies (cm^{-1}) and IR intensities (km/mol, in *parentheses*) for the ground state of **3** compared to other ab initio results and experimental data

Mode	CASSCF[a]	CCSD(T)[b]	MP2[c]	Expt.[d]
b_1	223 (3)	240 (3)	225 (<1)	
b_2	236 (2)	276 (1)	262 (1)	
b_1	985 (14)	1049 (19)	1051 (8)	1002 (17)
b_2	1050 (6)	1057 (3)	1080 (2)	
a_1	1118 (2)	1125 (2)	1152 (<1)	
a_1	1491 (5)	1503 (11)	1542 (3)	1446 (16)
a_1	2019 (263)	2019 (248)	2075 (170)	1952 (100)
a_1	3019 (12)	3146 (5)	3206 (5)	
b_2	3094 (2)	3210 (<1)	3304 (<1)	

[a] Calculations using the ANO-S C[4s3p2d]/H[3s2p] basis set
[b] cc-pVTZ basis set [14]
[c] 6-31G** basis set [11]
[d] Argon matrix, 8 K [14]

Table 15. CASSCF computed harmonic vibrational frequencies (cm^{-1}) and IR intensities (km/mol, in *parentheses*) for the ground state of **2**, compared to other ab initio results and experimental data

Mode	C_s **2**		Mode	C_2 **2**		
	CASSCF[a]	UMP2[b]		CASSCF[a]	CCSD(T)[c]	Expt.[d]
a''	282 (22)	343 (18)	b	170 (63)	132 (77)	249 (100)
a'	350 (3)	389 (7)	a	319 (<1)	242 (9)	
a''	403 (26)	477 (7)	b	334 (19)	334 (59)	
a'	460 (42)	561 (22)	a	382 (21)	412 (16)	403 (25)
a'	695 (19)	575 (8)	a	524 (30)	414 (15)	550 (50)
a'	1160 (11)	1226 (9)	a	1255 (<1)	1273 (0)	
a'	1651 (36)	1679 (23)	b	1527 (56)	1644 (10)	1621 (7)
a'	3221 (2)	3452 (7)	b	3270 (18)	3422 (86)	3265 (71)
a'	3343 (32)	3561 (26)	a	3279 (2)	3443 (3)	

[a] Calculations using the ANO-S C[4s3p2d]/H[3s2p] basis set
[b] Calculations using the 6-31G** basis set [13]
[c] Values obtained with the cc-pVTZ basis set [14]
[d] Argon matrix, 8 K [14]

Table 16. CASSCF computed harmonic vibrational frequencies (cm^{-1}) and IR intensities (km/mol, in *parentheses*) for the lowest triplet state of 1 compared to other ab initio results

Mode	CASSCF[a]	CCSD(T)[b]
a	585 (10)	720 (7)
a	646 (47)	599 (55)
a	889 (71)	920 (72)
a	928 (5)	935 (1)
a	998 (7)	995 (19)
a	1008 (42)	1089 (28)
a	1611 (8)	1673 (5)
a	2998 (36)	3125 (22)
a	3486 (15)	3344 (16)

[a] Calculations using the ANO-S C[4s3p2d]/H[3s2p] basis set
[b] TZP basis set [8]

Table 17. CASSCF computed harmonic vibrational frequencies (cm^{-1}) and IR intensities (km/mol, *in parentheses*) for the lowest triplet state, 1^3B_1, of **3** compared to other ab initio results

Mode	CASSCF[a]	CCSD(T)[b]	MP2[c]
b_2	258 (<1)	222 (<1)	406 (<1)
b_1	388 (3)	375 (3)	483 (1)
b_1	630 (43)	650 (61)	709 (24)
b_2	1039 (<1)	997 (7)	1076 (<1)
a_1	1095 (7)	1094 (6)	1150 (4)
a_1	1484 (<1)	1485 (0.0)	1528 (<1)
a_1	1901 (4)	1954 (<1)	2072 (1)
a_1	3060 (9)	3171 (3)	3280 (<1)
b_2	3150 (2)	3271 (<1)	3394 (<1)

[a] Calculations using the ANO-S C[4s3p2d]/H[3s2p] basis set
[b] TZP basis set [8]
[c] 6-31G** basis set [11]

diradical structure was suggested mainly on the basis of the better agreement obtained for the CH stretching vibrations. Thus, for a C_s carbene structure, with two different C—H bonds, MP2 theory predicted two bands of different wavelengths and with nonzero intensity (Table 15) [13], in disagreement with the experimental observation of one band, as shown by the experimental data listed in Table 15. The computed IR spectrum using the QCISD method for the C_2 structure [7] showed, however, only one band in the CH stretching vibration region since the symmetrical CH stretching mode was predicted to have a very low intensity and was located very close in energy to the active CH stretching vibration. On the other hand, Maier et al. [13] took into account the nonrigidity of **2** and used an anharmonic model for the calculation of the IR spectrum. These calculations were based on a C_s structure and the anharmonic treatment was only applied to two modes. The agreement with the observed IR spectrum was in this way improved, in particular for the modes related to the CC stretching vibrations, which were considerably reduced in intensity. However, in contrast with the experimental data, the computed IR spectrum still showed two allowed and separate transitions for the CH stretching vibrations; this was mainly attributed to the harmonic treatment performed for the remaining seven modes [13].

Table 18. CASSCF computed harmonic vibrational frequencies (cm^{-1}) and IR intensities (km/mol, in *parentheses*) for the lowest singlet state of **2**

C_s **2**		C_2 **2**	
Mode	CASSCF[a]	Mode	CASSCF[a]
a''	286 (1)	b	360i (475)
a'	354 (19)	b	250 (14)
a'	435 (57)	a	442 (15)
a''	769 (13)	a	866 (15)
a'	1039 (13)	a	939 (0)
a'	1107 (50)	a	1210 (<1)
a'	1981 (57)	b	1738 (7)
a'	2910 (48)	a	3121 (<1)
a'	3355 (35)	b	3125 (3)

[a] Calculations using the ANO-S C[4s3p2d]/H[3s2p] basis set

We computed the CASSCF harmonic vibrational frequencies for the triplet ground state of both the C_2 and C_s structures of **2**. The results are collected in Table 15 together with the experimental data [14]. For the sake of comparison, Table 15 also includes the harmonic vibrational frequencies obtained with the CCSD(T) method and the cc-pVTZ basis set for C_2 **2** [14] and those computed by Maier et al. [13] at the unrestricted MP2/6-31G** level for C_s **2**. The CCSD(T) method, in

combination with a TZP basis set, provides one imaginary frequency for the C_s structure of **2** [8], which has been, however, characterized as a minimum using the Møller–Plesset approach (MP2 and MP4) [7, 13], as well as by the present CASSCF calculations.

As Table 15 shows, there is agreement between the CASSCF and CCSD(T) frequencies of C_2 **2**, as found for the other isomers. The computed IR intensities are, however, quite different, with the CCSD(T) values closer to the experimental relative intensities, especially for the high-frequency modes. Thus, for instance, the CH stretching vibration computed at 3270 cm^{-1} is predicted by the CASSCF calculation to have a too low intensity in comparison with the experimental result. In contrast, the low-energy region of the observed IR spectrum is better reproduced by the CASSCF results of C_2 **2**. The CASSCF results give a too high intensity for the CC stretching mode of both structures, in disagreement with the experimental data (the mode with frequency 1527 cm^{-1} in C_2 **2** and 1651 cm^{-1} in C_s **2**). Summarizing, neither of the sets of harmonic vibrational frequencies and intensities presented in Table 15 show overall agreement with the observed IR spectrum, as could be expected on the basis of the nonrigidity predicted for **2**. The energy difference between the optimal C_2 and C_s forms of **2** was estimated to be less than 0.2 kcal/mol (70 cm^{-1}) at the CASPT2 level. Finally, the harmonic frequencies listed in Table 15 also indicate the floppiness of the structure since quite low values are predicted for some of the modes. For instance, the lowest frequency of both structures corresponds to a CH wagging mode.

The harmonic vibrational frequencies of both **4a** and **4b**, characterized as transition states in the singlet ground state, were also computed using the BS2 basis set. The results are presented in Table 19 together with the values obtained by Sherrill et al. [16] at the TCSCF and CCSD(T) levels of theory for **4b**.

The CASSCF frequencies computed for **4b**, as well as the relative intensities, agree with those obtained at the CCSD(T) level [16], except for the CH_2 twist mode. As previously discussed, this mode is found to have an imaginary value at the CCSD(T) level mainly due to the monoconfigurational character of the reference function used in the calculation. Thus, the frequency of the CH_2 twist mode acquires a real value when the two configurations which are important for describing the singlet ground state (see earlier) are taken into account, as shown by the TCSCF and present CASSCF results. Sherrill et al. [16] have also reported a value of 381 cm^{-1} for this frequency using a TC-CISD approach and a double-zeta polarized basis set.

The differences previously reported between **4a** and **4b** are also reflected in the computed IR spectra. Thus, for instance, the longer C_1—C_2 bond (Fig. 1) predicted for **4a** in comparison with **4b** results in a smaller value for the frequency of the symmetric CC stretching mode (935 versus 1055 cm^{-1}). Similarly, the frequency of the mode corresponding to the symmetric CC stretching vibration related to the multiple bond (C_2—C_2) has a smaller value, 1563 cm^{-1}, for **4a**, where the bond is better described as a double bond instead of as a weak triple bond as for **4b**. Furthermore, some mixing is found between the symmetric C_2—C_2 stretching and CH_2 scissor modes in **4a**, as a consequence of the quite close values determined for the frequencies (1563 and 1500 cm^{-1}, respectively). In **4b**, these two modes appear clearly separate owing to the higher frequency of the symmetric C_2—C_2 stretching vibration, which is computed to be 1825 cm^{-1}, with a negligible intensity in the IR spectrum.

The lowest triplet state, 1^3B_2 state, of **4b** is characterized as a minimum. The CASSCF harmonic vibrational frequencies and intensities are shown in Table 20.

4 Conclusions

An ab initio study, based on MC wave functions, has been presented for the singlet and triplet isomers of C_3H_2. Geometries, harmonic frequencies, and IR intensities are reported at the CASSCF level, while total and relative energies are obtained using CASPT2. Combined with the earlier studies, a rather complete picture has

Table 19. CASSCF computed harmonic vibrational frequencies (cm^{-1}) and IR intensities (km/mol, in *parentheses*) for the ground state of **4**, compared to other ab initio results

Planar **4**		Perpendicular **4**			
Mode	CASSCF[a]	Mode	CASSCF[a]	TCSCF[b]	CCSD(T)[c]
b_2	658*i* (2)	b_2	647*i* (611)	630*i* (597)	618*i* (520)
a_2[d]	272 (0)	a_2[d]	455 (0)	417 (0)	93*i* (0)
a_1[e]	935 (<1)	a_1[e]	1055 (107)	1180 (171)	1089 (119)
b_2	952 (<1)	b_1	1088 (<1)	1158 (2)	1075 (<1)
b_1	1001 (25)	b_2	1151 (2)	1236 (<1)	1137 (<1)
a_1	1500 (<1)	a_1	1608 (8)	1664 (17)	1539 (8)
a_1	1563 (27)	a_1	1825 (<1)	2049 (<1)	1874 (<1)
a_1	3204 (1)	a_1	3188 (56)	3246 (81)	3087 (46)
b_2	3333 (3)	b_1	3296 (8)	3324 (13)	3164 (9)

[a] Calculations using the ANO-S C[4s3p2d]/H[3s2p] basis set
[b] Results obtained with the double-zeta polarization basis set of Dunning [16]
[c] Results obtained with a TZ(2df,2dp) basis set [16]
[d] CH_2 twist
[e] Symmetric C—C stretch

Table 20. CASSCF computed harmonic vibrational frequencies (cm^{-1}) and IR intensities (km/mol, in *parentheses*) for the 1^3B_2 state of perpendicular, **4** compared to other ab initio results

Mode	CASSCF[a]	SCF[b]
b_2	640 (8)	773
a_2	726 (0)	895
a_1	877 (2)	1108
b_2	975 (55)	1142
b_1	1076 (3)	1171
a_1	1555 (<1)	1639
a_1	1648 (32)	1919
a_1	3194 (37)	3240
b_1	3306 (7)	3323

[a] Calculations using the ANO-S C[4s3p2d]/H[3s2p] basis set
[b] Results obtained with a DZP basis set [16]. The intensities were not reported in Ref. [16]

emerged of the bonding and relative stability of the different isomers of C_3H_2.

We predict the same order of stability for the singlet (**1s** > **3s** > **2s** > **4s**) and triplet (**2t** > **3t** > **1t** > **4t** > **5t**) states as most previous calculations. None of the structures, apart from **4b**, have significant MC character. They are, to 85% or more, dominated by one configuration, which justifies the similarity between the CASPT2 and CCSD(T) results. Apart from **2**, which has such a shallow potential-energy surface in the vicinity of the minima that the harmonic approximation might not be valid, the CASSCF, CCSD(T), and experimental vibrational frequencies deviate by less than 100 cm^{-1}.

The following summarizes the most relevant results obtained for the different isomers. The lowest singlet and triplet excited states of **1** do not have equilibrium geometries of C_{2v} symmetry. For both triplet and singlet **2**, the C_s and C_2 structures are almost degenerate. Both triplet structures are characterized as minima, but only the singlet C_s geometry is stable. The 1^1A_2 state of **3** has one imaginary frequency, while it was previously characterized as an equilibrium geometry. **4b** is a transition state with one imaginary frequency of b_2 symmetry, which supports the hypothesis that it participates in the automerization of **3**. **4a** has also been characterized as a transition state, which might be involved in the conversion of **3** to **1**.

Acknowledgements. The research reported in this communication has been supported by the European Commission through the TMR program (grant ERBFMRXCT960079), by the Swedish Natural Science Research Council (NFR), and by the project PB97-1377 of the Spanish DGES-MEC.

References

1. DeFrees DJ, McLean AD (1986) Astrophys J 308: L31
2. Kanata H, Yamamoto S, Saito S (1987) Chem Phys Lett 140: 221
3. Cooper DL, Murphy SC (1988) Astrophys J 333: 482
4. Takahashi J, Yamashita K (1996) J Chem Phys 104: 6613
5. Bernheim RA, Kempf RJ, Gramas JV, Skell PS (1965) J Chem Phys 43: 196
6. Jonas V, Böhme M, Frenking G (1992) J Phys Chem 96: 1640
7. Herges R, Mebel A (1994) J Am Chem Soc 116: 8229
8. Ochsenfeld C, Kaiser RI, Lee YT, Suits AG, Head-Gordon M (1997) J Chem Phys 106: 4141
9. Seburg RA, DePinto JT, Patterson EV, McMahon RJ (1995) J Am Chem Soc 117: 835
10. Reisenauer HP, Maier G, Riemann A, Hoffmann RW (1984) Angew Chem Int Ed Engl 23: 641
11. Maier G, Reisenauer HP, Schwab W, Cársky P, Hess BA Jr, Schaad LJ (1987) J Am Chem Soc 109: 5183
12. Lee TJ, Bunge A, Schaefer HF III (1985) J Am Chem Soc 107: 137
13. Maier G, Reisenauer HP, Schwab W, Cársky P, Spirko V, Hess BA Jr, Schaad LJ (1989) J Chem Phys 91: 4763
14. Seburg RA, Patterson EV, Stanton JF, McMahon RJ (1997) J Am Chem Soc 119: 5847
15. Hehre WJ, Pople JA, Lathan WA, Random L, Wasserman E, Wasserman ZR (1976) J Am Chem Soc 98: 4378
16. Sherrill CD, Brandow CG, Allen WD, Schaefer HF III (1996) J Am Chem Soc 118: 7158
17. Mebel AM, Jackson WM, Chang AHH, Lin SH (1998) J Am Chem Soc 120: 5751
18. Bofill JM, Farrás J, Olivella S, Solé A, Vilarrasa J (1988) J Am Chem Soc 110: 1694
19. Stanton JF, DePinto JT, Seburg RA, Hodges JA, McMahon RJ (1997) J Am Chem Soc 119: 429
20. Jackson WM, Mebel AM, Lin SH, Lee YT (1997) J Phys Chem A 101: 6638
21. Borden WT, Davidson ER (1979) Annu Rev Phys Chem 30: 125
22. Olsson MHM, Borowski P, Roos BO (1996) Theor Chim Acta 93: 17
23. Roos BO (1987) In: Lawley KP (ed) Advances in chemical physics: ab initio methods in quantum chemistry II. Wiley, Chichester, p 399
24. Andersson K, Malmqvist P-Å, Roos BO, Sadlej AJ, Wolinski K (1990) J Phys Chem 94: 5483
25. Andersson K, Malmqvist P-Å, Roos BO (1992) J Chem Phys 96: 1218
26. Bernhardsson A, Lindh R, Olsen J, Fülscher M (1999) Mol Phys 96: 617
27. Andersson K (1995) Theor Chim Acta 91: 31
28. Pierloot K, Dumez B, Widmark P-O, Roos BO (1995) Theor Chim Acta 90: 87
29. Widmark P-O, Malmqvist P-Å, Roos BO (1990) Theor Chim Acta 77: 291
30. Andersson K, Blomberg MRA, Fülscher MP, Karlström G, Lindh R, Malmqvist P-Å, Neogrády P, Olsen J, Roos BO, Sadlej AJ, Schütz M, Seijo L, Serrano-Andrés L, Siegbahn PEM, Widmark P-O (1997) MOLCAS version 4.0. Department of Theoretical Chemistry, University of Lund, Sweden
31. Bogey M, Demuynck C, Destombes JL, Dubus H (1987) J Mol Spectrosc 122: 313
32. Robinson MS, Polak ML, Bierbaum VM, DePuy CH, Lineberger WC (1995) J Am Chem Soc 117: 6766
33. Stanton JF, Byun KS (1999) Mol Phys 96: 505
34. Saxe P, Schaefer HF III. (1980) J Am Chem Soc 102: 3239
35. Seburg RA, McMahon RJ (1995) Angew Chem Int Ed Engl 34: 2009